COMMISSIONING RESULTS OF THE HZB QUADRUPOLE RESONATOR

R. Kleindienst*
A. Burrill, S. Keckert, J. Knobloch, O. Kugeler
Helmholtz-Zentrum-Berlin, Albert-Einstein-Strasse 15, 12489 Berlin, Germany

Abstract

Recent cavity results with niobium have demonstrated the necessity of a good understanding of both the BCS and residual resistance. For a complete picture and comparison with theory, it is essential that one can measure the RF properties as a function of field, temperature, frequency and ambient magnetic field. Standard cavity measurements are limited in their ability to change all parameters freely and in a controlled manner. On the other hand, most sample measurement setups operate at fairly high frequency, where the surface resistance is always BCS dominated. The quadrupole resonator, originally developed at CERN, is ideally suited for characterization of samples at typical cavity RF frequencies. We report on a modified version of the QPR with improved RF figures of merit for high-field operation. Experimental challenges in the commissioning run and alternate designs for simpler sample changes are shown alongside measurement results of a large grain niobium sample.

INTRODUCTION

Bulk niobium cavities today can achieve quality factors of over 10^{10} at accelerating gradients of $25-35$ MV/m. These high quality cavities can be produced consistently with a high success rate as the result of decades of research into the material properties of niobium and the required surface finishing and heat treatment techniques.

Three paths are currently being pursued to break beyond bulk niobium cavities:

- Titanium or nitrogen 'doped' niobium
- Different superconductors such as Nb_3Tn, NbN or MgB_2, coated on copper or niobium
- A SIS multilayer structure, described in [1]

For all of these approaches, studying samples as opposed to cavities can be advantageous. Thin films deposition is easier on flat samples as opposed to on curved surfaces. The cost of a small sample and the potentially fast turn-around rate are further benefits. Lastly, cavity testing is typically limited to a narrow temperature range below 4.2 K.

RF Sample Testing Setups

Several systems exist around the world dedicated to testing the RF properties of superconducting samples. At Cornell, a third generation TE host cavity has been commissioned, which at 4 GHz can apply 80 mT onto a flat sample of 10 cm diameter [2, 3] . A temperature mapping system on the back of the sample is used to measure the RF losses. A similar system is in operation at Orsay/Saclay [4]

At JLAB, a sapphire loaded cavity has been used to characterize 5 cm samples at 7.5 GHz. [5]. The sample is thermally decoupled from the cavity, allowing measurements within the temperature range between 2 and 20 K.

The quadrupole resonator was developed at CERN in the late 1990's [6]. Since its upgrade, it can be used to characterize a superconducting sample at 400 , 800 and 1200 MHz [7]. Measurements are possible over a wide temperature range with peak magnetic fields reaching up to 60 mT on the 7.5 cm sample.

The benchmarks of the different systems are summarized in Table 1. At HZB, the decision to build an improved version of the QPR was made due to advantageous measurement frequencies. At the comparatively low frequency, one can not only study the BCS resistance, but also the residual resistance of a sample. Having multiple frequencies also allows measuring scaling factors and provides additional cross checks to the data. The main aims for improvement of the system were identified as raising the peak field on sample, while increasing measurement resolution and the change of sample. The size of the sample was left unchanged, to allow interchangeability between the two systems.

Overview Quadrupole Resonator

Figure 1 shows a cross sectional view of the Quadrupole Resonator (QPR). With the particular geometry of the niobium rods, a set of TE21n modes exist, which all have high magnetic field region on the sample surface.

The sample plate of diameter 75 mm is welded to a hollow niobium tube which is brazed to a double sided stainless steel flange. The coaxial gap between the resonator and the sample chamber causes dipole and quadrupole modes to decay exponentially when penetrating towards the flange.

The coaxial gap separating sample and resonator also decouples them thermally. This allows changing the sample temperature freely while keeping the rest of the resonator at the temperature of the helium bath, typically 1.8 K.

* Email: raphael.kleindienst@helmholtz-berlin.de

ISBN 978-3-95450-178-6

Table 1: Comparison of Surface Impedance Characterization Setups

System	Sam ∅ [cm]	Freq [GHz]	Measurement	B_{Sam}[mT]
Cornell TE011	7.0	4.0	Thermometric	80
Mushroom TE012/013	9.5	4.78/6.16	RF Measurement	60
Orsay/Saclay TE011	13	3.88/5.12	RF/thermomemtric	25
JLAB Sapphire loaded	5.0	7.5	Calorimetric	20
CERN QPR	7.5	0.4/0.8/1.2	Calorimetric	60
HZB QPR	7.5	0.43/0.85/1.3	Calorimetric	120

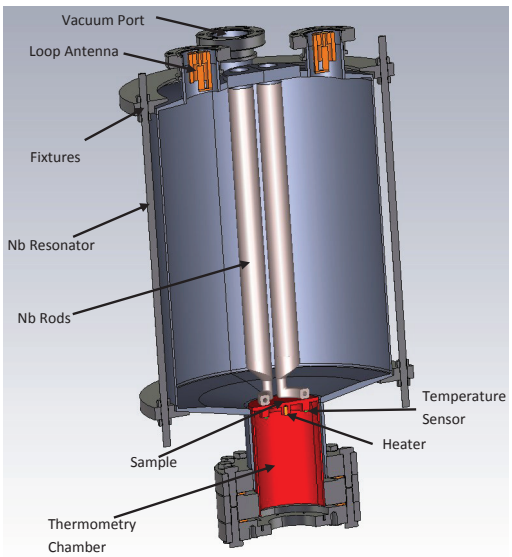

Figure 1: Schemata of the QPR. Not included in the diagram are the solenoid and the magnetometer within the thermometry chamber.

Measurement Principle Using the heater and the temperature sensors underneath the sample, the temperature of the sample can be varied between 1.8 K and ~ 15 K. In our setup, a Lakeshore temperature controller (LS336) is used to stabilize the temperature within ±0.1 mK at 2 K.

To measure the surface resistance of the sample, a compensation technique is used [7]: First, the sample is heated to the desired temperature and the heater power (P_1) is determined by measuring the voltage across the heater. RF power is then coupled into the QPR, dissipating additional RF power into the sample. The temperature controller reduces the power to the heater necessary to stabilize the temperature of the sample at an unchanged value. Once the conditions are stationary, the heater power is measured again (P_2). If one assumes that the total power required to keep the temperature constant is also constant, one has:

$$P_{RF} = P_2 - P_1 = \frac{1}{2}\int_{Sample} R_S\,|H|^2\,dA \qquad (1)$$

Introducing an average surface resistance $\widetilde{R_S}$ one obtains:

$$\widetilde{R_S} = \frac{2(P_2 - P_1)}{\int_{Sample} |H|^2\,dA} \qquad (2)$$

The measurement technique is summarised in Figure 2.

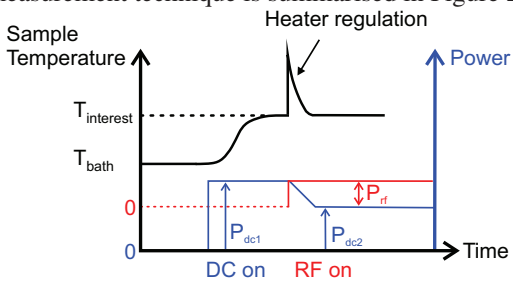

Figure 2: Illustration of the measurement principle. [8]

From here, one still needs to determine the integral in the denominator. This is done by measuring the stored energy in the resonator with a calibrated field probe and using a simulation parameter c, which quantifies how strongly the magnetic fields are focused on to the sample : $c = \frac{\int_{Sample}|H|^2 dA}{U}$

RF Optimization Starting with the geometry of the original CERN Quadrupole Resonator adapted to include a 1.3 GHz mode as a baseline, an RF optimization was performed. The aim was to establish a design for measurements at high fields and with a high resolution. Therefore, the aim was to improve peak field ratios as well as increase the focussing factor c established earlier. A detailed account of the optimization process, is given in [9]. The results of the RF optimization are shown in Table 2. Here, B_{Sam} refers to the peak field on the sample, while E_{pk} and B_{pk} refer to the peak field on any surface of the resonator. The two largest changes made to the geometry were increasing the thickness of the niobium rods from 8 mm to 13 mm and reducing the gap between rods and sample to 500 μm. The curvature of the loops and the transition between rods and loops was also altered.

Table 2: Comparison of RF Figures of Merit

	Baseline	Optimized
c	$5.15 \cdot 10^7$ A^2/J	$1.12 \cdot 10^8$ A^2/J
B_{sam}/E_{pk}	4.68 mT/(MV/m)	7.44 mT/(MV/m)
B_{sam}/B_{pk}	.81	.89

The increased focusing factor c means that at a constant stored energy in the cavity, the RF losses over the sample will be higher in the optimized design, increasing the measurement resolution. The reduced peak fields reduce the risk

ISBN 978-3-95450-178-6

of field emission and increase the achievable peak magnetic field on the sample surface.

Construction and Surface Finish Based on the optimized RF design, the HZB QPR was built by Niowave in 2013. In comparison to the CERN version, some changes were made to the outer mechanical design, such as omitting the flange in the middle of the resonator and decreasing the wall thickness to 2 mm. While these measures reduced the cost significantly, the decreased stiffness of the resonator did cause some issues during the first measurements.

The resonator and the rods were made of fine grain, RRR 300 Niobium. The rods are hollow, with a wall thickness of 3 mm, for efficient cooling by liquid helium. The sample chamber was made from large grain, RRR 300 Niobium and brazed to the stainless steel flange connecting it to the resonator.

After production, the QPR went through the standard surface finishing procedures for niobium cavities at Jefferson Lab:

- 150 μm BCP, measured with an ultrasonic thickness gauge at the cylinder wall
- 600 °C High temperature bake for 12 h
- High Pressure Rinse with 55 bar jet shooting upwards through the rods from the below the loops
- 20 μm light - BCP
- 120 °C low temperature bakeout for 48 h

After the treatments, the QPR was tested in the Vertical Test Facility at JLab, where peak fields up 100 mT were reached on the sample.

EXPERIMENTAL CHALLENGES DURING COMMISSIONING

Three main experimental challenges were encountered when commissioning the QPR at HZB. The first is the susceptibility of the geometry multipacting, the second concerns frequency detuning cause by mechanical vibrations. Additionally, pulsed measurements, needed to measure the surface resistance of the sample across the entire parameter space, are discussed in this section.

Multipacting

Multipacting is the resonant electron discharge, during which an initial seed electron is accelerated by the RF field against cavity wall, creating secondary electrons. If the emission is synchronized with the RF fields, this can cause the secondary electrons to be accelerated again and emit further electrons, leading to an exponential growth of the number of electrons. In this case, power supplied to the cavity is dissipated by the electrons, limiting the microwave field to a certain threshold.

In the case of the Quadrupole Resonator, potential locations for multipacting are the narrow gap between sample and rods as well as between the rods at half the vertical height of the resonator, where the magnetic fields disappear. In both regimes, the electric field can be described by $E = E_0 sin(\omega t)$ and the equation of motion of an electron is given by:

$$\ddot{x} = \frac{eE_0}{m} sin(\omega t) \tag{3}$$

The multipacting barriers can be calculated analytically, by imposing a boundary condition that emitted electrons reach the other side of the gap at odd integer numbers of the half RF period. Furthermore, the impact energy of the electrons has to be between 100 and 1000 eV, as only in this case more than one secondary electron is emitted on average by a heat-treated niobium surface [10]. For a gap of length L and order of multipacting n, the gap voltage V is [11]:

$$V = L \cdot E_0 = \frac{4\pi m}{e} \frac{L^2 f^2}{(2n-1)} \tag{4}$$

from which the impact energy can be calculated. Between sample and rod, the gap is so narrow that electrons cannot reach dangerous impact energies before hitting the opposing sides. For the case between the rods we have:

Table 3: Two Point Multipacting Barriers between Niobium Rods

Order n	Impact Energy [eV]	E_0[kV/m]
1	2767	241
2	922	80.5
3	553	48.3
4	395	34.5
15	95.4	8.3

We see that there are many orders of multipacting producing potentially dangerous electrons. All of these barriers occur at very low fields,for the $n = 2$ case, the peak magnetic field on the sample is below 2 mT.

During commissioning multipacting was repeatedly observed. It did not limit performance however as the barriers could be processed away by applying RF for several hours.

Mechanical Susceptibility

For the CERN Quadrupole resonator it was reported that microphonic oscillations of the niobium rods at 69 Hz caused difficulties during measurements, particularly at higher frequencies. [7]. We expected these difficutlies to be reduced with the HZB design, as the niobium rods became slightly shorter (due to the frequency change from 400 MHz to 433 MHz as well as wider as a result of the RF optimization. Mechanical simulations predicted the lowest modes to be at 120 Hz.

During the first tests at HZB, the fields attainable in the QPR were limited to around 30 mT in CW mode and 60 mT in pulsed mode. At higher field levels, the frequency detuning could not be compensated by the phase-lock loop. In the CW limit, it was observed that the detuning signal fed from the PLL to the voltage controlled oscillator continuously

increased over the period of some tens of second. At one point, the detuning signal exceeded the bandwidth of VCO, after which the field collapsed. As seen in Figure 3, the problem was not caused by thermal runaway on the sample surface.

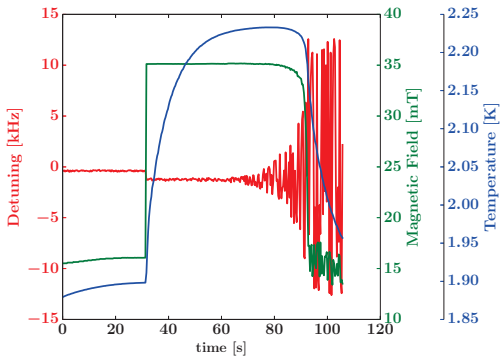

Figure 3: Frequency detuning (red) shown together with peak magnetic field and temperature of the sample.

Taking the fourier transform of the detuning signal yields the microphonics spectrum. It shows a prominent peak at 100 Hz. That the 100 Hz contribution is the cause of the field limitation becomes particularly clear, if the rising detuning signal is split up as shown in Figure 4.

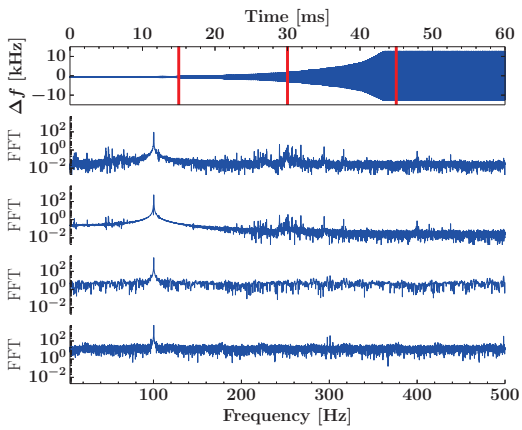

Figure 4: Microphonics spectrum at various stages during rising detuning. The top graph shows the detuning signal in time domain. Below, from top to bottom are the microphonics spectra of the four sections delimited by the red vertical lines.

The strong detuning observed indicate the susceptibility of the QPR to mechanical effects. A very large value for $df/dp = -3\,\mathrm{kHz/mbar}$ was measured as well as a Lorentz force detuning coefficient of $-1.85\,\mathrm{Hz/mT^2}$. Coupled mechanical-RF simulations showed that the Lorentz force detuning was primarily caused by the Lorentz pressure pushing the rods apart at the lower end.

Geophone Measurements For further mechanical analysis, the mechanical modes of the QPR were measured in the warm state with a geophone. A geophone consists of a spring mounted coil with an iron core rigidly mounted to the outer case [12]. Vibrations passed onto the outer case, which was connected with screws to a top flange of the QPR, cause an induced voltage proportional to the velocity. Integrating this signal and taking the Fourier transform yields the microphonics spectrum. The spectrum was recorded several times with mechanical excitations at different locations, giving a possibility to locate the mechanical modes. The modes seen with the geophone match those of the microphonics measurement, shifted by several Hz due to the different elasticity of the niobium in the warm and cold state. An important result is that several mechanical modes seem to exist around 100 Hz as seen in Figure 5.

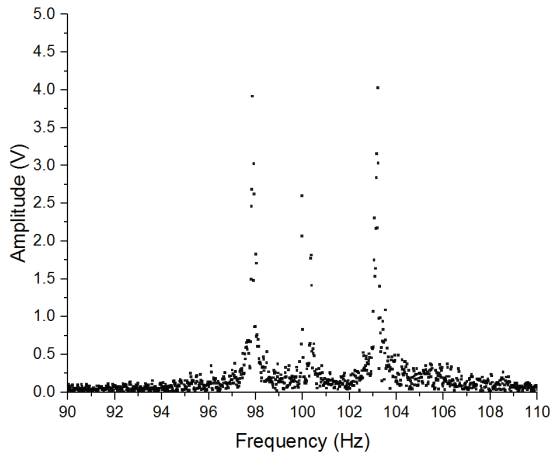

Figure 5: Mechanical spectrum measured with a geophone around 100 Hz.

High Field Operation The microphonics spectrum paired with the geophone measurement clearly indicate that vibrations of the rods at 100 Hz were the most likely cause for the field limitation in the initial tests at HZB. Additionally, the 100 Hz also appeared prominently in the spectrum of the signal generator. It is likely that 100 Hz noise excited mechanical oscillations of the rods at the same frequency, causing a resonance runaway.

As a countermeasure, the bandwidth of the resonator was increased by increasing the coupling, signal generator and pulse generator were swapped to lower noise models and the mechanical fixtures holding the resonator were tightened. In the next run, the peak field was not limited by microphonics, but through a quench at 120 mT peak field on sample. The quench was reproduced several times, the temperature on the sample not spiking upwards indicates the location of the quench to be on the niobium rods.

Pulsed Measurements

Heat dissipated on the sample surface has to flow down the entire sample chamber and through the stainless steel flange before reaching the helium bath. This results in a significant temperature increase on the sample surface, even at

ISBN 978-3-95450-178-6

low/medium fields. For the surface resistance measurement this means that not the entire parameter space can be mapped using a CW measurement, as the compensation technique does not work if the RF fields already heat the sample above the temperature of interest.

The solution to this problem is using pulsed RF fields. The measurement principle remains almost unchanged, equation 2 has only to be modified by multiplying in the duty factor. Figure 6 shows the maximum duty cycle usable to measure the surface resistance at a given (T,B) combination. For high fields and low temperatures, pulsed measurements are always necessary.

Pulsed measurements have three potential sources of error. The first is related to the rise and fall time of the fields in the cavity. The characteristic time constant is given by $\tau = \frac{Q_L}{\omega}$, which at 416 MHz and with a loaded quality factor in the range of 10^6 is around 2 ms. An error can occur if this time constant is significant compared to the pulse period.

The second source of error occurs when the temperature on the sample surface varies significantly between the RF pulses. A constant reading on the temperature sensor does not guarantee that the surface temperature is constant as well, as temperature variations can be smeared out across the thickness of the sample. Transient thermal simulations have been performed, but are difficult to interpret, as they strongly depend on the heat capacity of the niobium, which is extremely temperature dependent at low temperature.

The third error source is caused by a temperature gradient across the sample. Simulations show, that the central heater produces a significant temperature gradient across the sample, whereas the RF fields produce a very homogeneous temperature distribution. Lowering the duty cycle increases the heater power required to maintain the temperature of interest and thereby increases the temperature gradient. As the magnetic field is highly inhomogeneous across the sample, this potentially changes the RF losses. Note that this is a general problem - measuring at higher fields without changing the duty cycle leads to a reduced gradient and thus a systematic error. For future measurement runs it is planned to use a ring shaped heater which produces almost no temperature gradient.

Experimentally, it was found that both the pulse period and the duty cycle can effect the surface resistance measurement. For low temperature and fields, this effect was observed to be significant, for higher RF losses the pulse setting did not have an effect on the measured surface resistance. This is shown in Figure 7. As a consequence, pulse period and duty cycle of the measurements shown in the subsequent sections were fixed at 131 ms and 30 %.

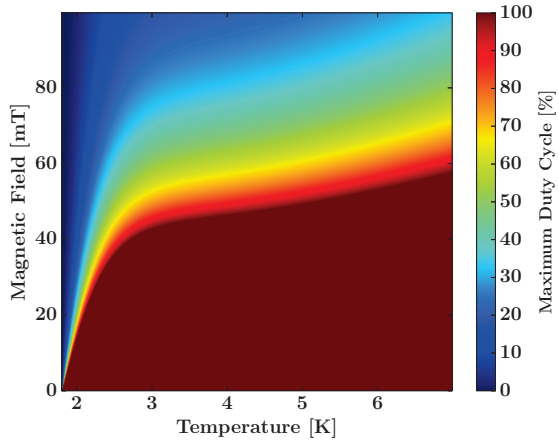

Figure 6: Maximum Duty Cycle useable for RF-DC measurement. The generic formula for niobium surface resistance is taken from [13], a residual resistance of 3 nΩ is assumed.

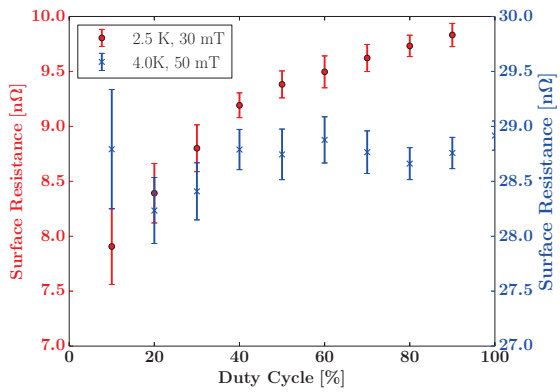

Figure 7: Surface Resistance measured against Duty cycle for low and high RF losses.

CHARACTERIZATION OF A LARGE GRAIN NIOBIUM PROBE

The first probe used to commission the QPR was made of large grain, RRR300 Niobium. The sample went through the standard procedure for surface finishing, including a 150 μm buffered chemical polishing (BCP), an 800 °C bake as well as a 120 °C low temperature bake.

RF Losses against Field Figure 8 shows the surface resistance measured against temperature for various temperatures at 416 MHz. The most salient feature visible is the decreasing surface resistance from 50 – 70 mT. At higher temperatures, the surface resistance does not decrease at this field range, but still goes through a point of inflection. Whether this feature is due to the material properties or due to a systematic error of the measurement is uncertain at this point.

The error bars increase strongly at low fields, as the RF-losses on the sample decrease and difference in the heater

voltages drops to the noise floor of the voltmeter. At medium and high fields, the statistical error of the measurement becomes very small, a significant systematic error is always present due to power meter error as well as uncertainty of the simulation constants.

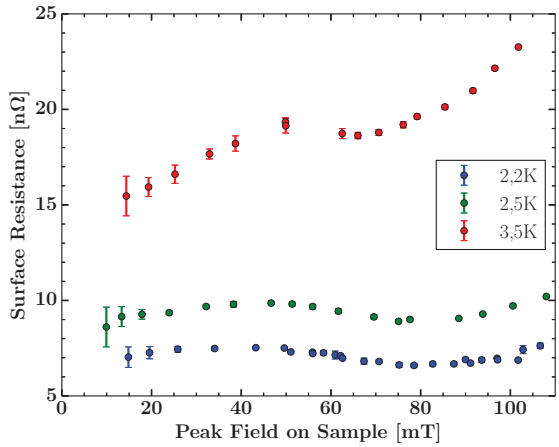

Figure 8: Surface Resistance against peak magnetic field on sample for different temperatures.

Trapped Flux Studies Trapped magnetic flux contributes significantly to the residual resistance in superconducting cavities [14]. These additional losses occur as magnetic flux lines present during the superconducting transition, are not expelled from the material entirely as predicted by the Meissner effect, but can remain trapped with efficiencies of up to 100 % [15]. To study this phenomenon, a copper solenoid was mounted under the sample, with a fluxgate magnetometer placed inside it. For measurements, the sample was heated to 11 K, an ambient field applied and the sample then cooled through the transition temperature before turning off the current passing through the coil. A higher reading of the magnetometer at this point compared with the initial reading are evidence of the incomplete Meissner effect. This process is shown in Figure 9. Note that the field produced by the heater is also seen by the magnetometer.

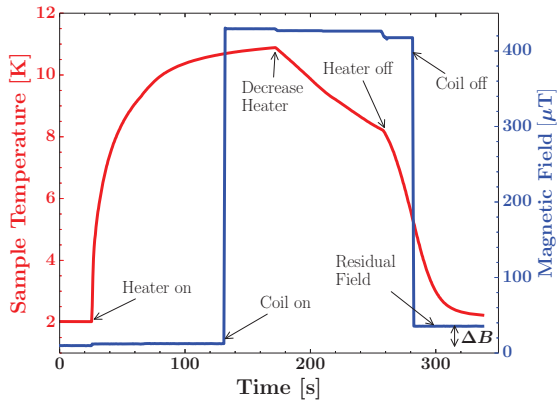

Figure 9: Sample temperature and reading of fluxgate magnetometer during thermal cycle with field cooldown.

Apart from the amount of flux trapped, one can also manipulate the cooling rate with which the sample passes through T_C, which has been shown to influence the residual resistance in superconducting cavities [16]. For the initial measurements, the cavity was always heated to 11 K, after which the heater was switched off completely. This created the same cooldown condition, the current flowing through the solenoid being the only variable. Figure 2 shows the surface resistance, measured at 2.5 K and 20 mT, for different residual fields. Note that this residual field is only the field measured by the magnetometer, which is proportional but not identical to the remaining field at the sample surface.

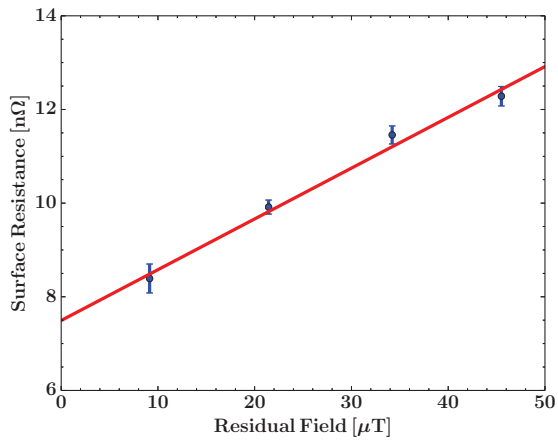

Figure 10: Surface resistance at 25 K and 20 mT against remnant magnetic field.

Critical Field Measurements The RF critical field of the sample can be measured by applying RF pulses with very low duty cycle and increasing amplitude. A quench can be identified by the pulse shape of the transmitted power pulse. To make sure that the quench occurs on the sample, it has to be heated to a temperature considerably above that of the helium bath.

ISBN 978-3-95450-178-6

Measuring the critical temperature for several temperature and assuming the typical $B_C(T) = B_{C0}\left(1 - \left(\frac{T}{T_C}\right)^2\right)$ scaling, one can now plot the critical field against T^2 and extract $B_{C,RF}$ from the y intercept of the fit. For the studied niobium sample, the RF critical field was found to be around 230 mT, as shown in Figure 11. This value is significantly higher than the 180 mT of B_{C1}, but nicely matches the values for the superheating fields found in [17]. The critical temperature derived from the fit is 9.32 K.

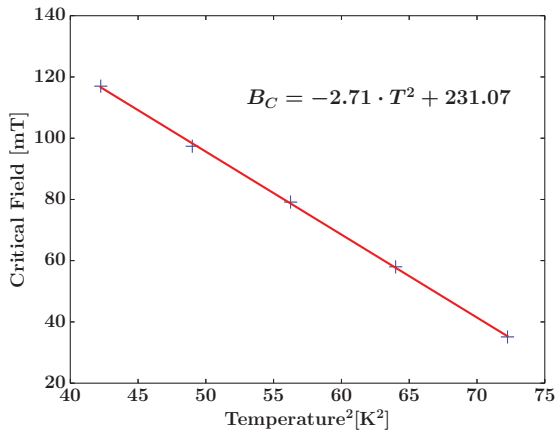

Figure 11: Critical Field measurement at 416 MHz.

OUTLOOK

The QPR at HZB has successfully been commissioned and has demonstrated that it can be a useful tool for studying superconducting samples.

Further improvements to the system are planned, such as using a demountable sample [18], reducing the temperature gradient over the sample with a different heater and expanding the measurement to include 850 MHz and 1300 MHz.

ACKNOWLEDGEMENTS

We would like to thank Dirk Pflueckhahn, Sascha Klauke, Stefan Rotterdam and Michael Schuster for their support in setting up the experiment at HZB. Thanks also to Steven Castagnola and his team for helping with the surface treatments and Tom Powers for performing the vertical test at Jefferson Laboratory.

This work was partly funded through EuCARD-2 under Capacities 7th Framework Programme, Grant Agreement 312453.

REFERENCES

[1] A. Gurevich, "Enhancement of rf breakdown field of superconductors by multilayer coating," *Appl. Phys. Lett. 88*, 2006.

[2] D. Hall, M. Liepe, D. Gonella, and M. I.S, "Srf material performance studies using a sample host cavity," in *IPAC 2014*, 2014.

[3] J. Maniscalco, D. Hall, and M. Liepe, "Rf performance studies of thin film superconductors using a sample host cavity," in *IPAC 2015 proceedings*, 2015.

[4] G. Martinet, "Development of a te011 cavity for thin-films study," in *Proceedings of SRF2009*, 2009.

[5] B. P. Xiao, C. E. Reece, H. L. Phillips, R. L. Geng, H. Wang, F. Marhauser, and M. J. Kelley, "Note: Radio frequency surface impedance characterization system for superconducting samples at 7.5 ghz," *Review of Scientific Instruments*, vol. 82, no. 5, pp. –, 2011.

[6] E. Haebel, E. Brigant, and E. Mahner, "The quadrupole resonator, design considerations and layout of a new instrument for the rf characterization of superconducting surface," in *6th European Particle Acceleartor Conference*, 1998.

[7] T. Junginger, *Investigations of the surface resistance of superconducting materials*. PhD thesis, University of Heidelberg, 2012.

[8] S. Aull, S. Doebert, T. Junginger, and J. Knobloch, "High resolution surface resistance studies," in *SRF 2013*, 2013.

[9] R. Kleindienst, J. Knobloch, and O. Kugeler, "Development of an optimized quadrupole resonator at hzb," in *Proceedings SRF 2013*, 2013.

[10] R. Calder, G. Dominichini, and N. Hilleret, "Influence of various vacuum surface treatments on the secondary electron yield of niobium," *Nucl. Instrum. Methods Phys. Res., Sect. B*, 1986.

[11] R. Parodi, "Multipacting," *arxiv.org*, 2011.

[12] A. Bertolini, "Vibration diagnostics instrinstrument for ilc," *Measurement Science and Technology*, 2007.

[13] H. Padamsee, J. Knobloch, and T. Hays, *RF Superconductivity for Acceleartors*. Wiley-VCH, 2008.

[14] C. Vallet, M. Bolore, B. Bonin, J. Charrier, B. Daillant, J. Gratadour, F. Koechlin, and S. H., "Flux trapping in superconducting cavities," in *Proceedings EPAC 1992*, 1992.

[15] S. Aull, O. Kugeler, and J. Knobloch, "Trapped magnetic flux in superconducting niobium samples," *Phys. Rev. ST Accel. Beams*, vol. 15, p. 062001, Jun 2012.

[16] J. Vogt, O. Kugeler, and J. Knobloch, "High-q operation of srf cavities: The potential impact of thermocurrents on the rf surface resistance," *PRSTAB-AB*, 2014.

[17] T. Hays and H. Padamsee, "Measuring the rf critical field of pb, nb, and nb3sn," in *Proceedings of SRF 1997*, 1997.

[18] S. Keckert, R. Kleindienst, J. Knobloch, and O. Kugeler, "Design and first measurement of an alternate calorimetry chamber for the hzb quadrupole resonator," in *Proceedings of SRF 2015, TUPB067*, 2015.